

## SURFACES OF HIGH- $T_c$ SUPERCONDUCTORS STUDIED BY MEANS OF THE SCANNING TUNNELING MICROSCOPE

A. WITEK, L. ORNOCH, A. DĄBKOWSKI and J. RAUŁUSZKIEWICZ

Institute of Physics, Polish Academy of Sciences, Warszawa

**ABSTRACT.** Observations of the natural surface of  $\text{BiSrCaCu}_2\text{O}_x$  sintered ceramics applying the scanning tunneling microscope are reported. Measurements were performed in air at room temperature. It can be deduced from the surface images, on which the growth steps are visible with heights corresponding to the dimension of the unit cell along the  $c$ -axis or its multiples, that the bulk orthorhombic structure extends to the surface. The surface investigated is rather clean, inert and metallic in nature. It can be identified as the Bi-O layer.

PACS no. 61.16.Di. 74.70.Vy.

### 1. INTRODUCTION

Since Binnig and Rohrer [1] built their first scanning tunneling microscope (STM), the number of applications of STM has multiplied tremendously. The STM probes the electronic properties of a surface, with images corresponding to contours of constant electronic densities of states. For metals, these contours usually reflect the surface potential barrier, which closely follows the surface atomic positions. For surfaces semiconducting in nature, however, the electronic densities of states (DOS) and their spatial distributions may depend sensitively on both the chemical identity and the position of the surface atoms.

The intriguing properties of high- $T_c$  oxide superconductors have also stimulated studies of their surface structure by STM technique. First experiences with contact resistance effects in various electrical measurements suggested the presence of surface layers with a composition and crystal structure different from those of the bulk. Similar conclusions could be drawn from the uncertainty of the superconducting energy gap measured by electron tunneling spectroscopy when only the local properties of surface are probed.

The surface properties of high- $T_c$  superconductors are important not only from the point of view of physical phenomena but also from that of possible applications. Superconducting shielding currents are generated on the surface of the material within the penetration depth; thus the distribution and intensities of

these currents are influenced by the electronic and crystallographic structures in the surface region. Studies of ceramic superconductors by means of a scanning tunneling microscope (STM) may then give insight into the atomic arrangements on the surface and eventually into the electronic density of states (DOS) at grain or twin boundaries.

The STM observations of Y–Ba–Cu–O superconductor by Garcia *et al.* [2] have suggested that the surface has a more or less semiconducting character with the exception of isolated strings on the surface which are metallic in nature. These metallic strings have been claimed to be twin boundaries and their role for superconductivity is essential. Thus it was interesting to examine the surface of  $\text{BiSrCaCu}_2\text{O}_x$  from this point of view.

It is worthwhile to note that many surface techniques working in vacuum can influence the surface properties of oxide superconductors due to the high mobility of oxygen atoms in the lattice. Our STM unit, which operates under atmospheric pressure when the oxygen content in the surface layer is at equilibrium with the oxygen in the air, does not cause oxygen depletion features.

The topographic images of  $\text{YBa}_2\text{Cu}_3\text{O}_7$  have been studied by van de Leemput *et al.* [3], Laiho *et al.* [4] and Okoniewski *et al.* [5]. In this paper we report observations of surface images of  $\text{BiSrCaCu}_2\text{O}_x$  ceramic. We have obtained reproducible topographic data on the surface of  $\text{BiSrCaCu}_2\text{O}_x$  resolving clearly the growth steps with step heights being multiples of the unit cell dimension in accordance with the X-ray crystallographic data [6].

## 2. MATERIAL

Samples of  $\text{BiSrCaCu}_2\text{O}_x$  were synthesized by standard solid-state reaction in the following steps: A mixture of appropriate amounts of  $\text{Bi}_2\text{O}_3$ ,  $\text{SrO}_3$ ,  $\text{CaO}_3$  and  $\text{CuO}$  weighted for the stoichiometry  $\text{Bi} : \text{Sr} : \text{Ca} : \text{Cu} = 1 : 1 : 1 : 2$  was sintered in air at  $860^\circ\text{C}$  in an alumina crucible, rehomogenized by crushing, regrinding and annealing at the same temperature for 4 hours. The annealed material was cooled down at about  $100^\circ\text{C}/\text{h}$ . Sintered pellets were cut into bar samples on which resistivity, magnetic susceptibility and X-ray diffraction studies were performed. The results of these studies will be published elsewhere. Here we only note that the critical temperature  $T_c$  determined from magnetic susceptibility measurements was 80 K. From X-ray analysis the dimensions of the orthorhombic unit cell were estimated as  $a = 5.3965 \text{ \AA}$ ,  $b = 5.4467 \text{ \AA}$  and  $c = 30.6735 \text{ \AA}$  with better fitting to the unit cell with superstructure  $a = 5.3980 \text{ \AA}$ ,  $b = 27.2516 \text{ \AA}$  and  $c = 30.6738 \text{ \AA}$  [6].

STM images of  $\text{BiSrCaCu}_2\text{O}_x$  samples were taken on the natural surfaces of the samples without any special cleaning procedures.

## 3. SCANNING TUNNELING MICROSCOPE

The scanning tunneling microscope used in our experiments was a slightly modified version of that described by Smith [7]. The modification consists in the

application of a bimorphic membrane as a  $z$ -piezodrives for the fine distance control with a sensitivity of  $100 \text{ \AA/V}$ . This membrane consisted from two circular piezoelectric plates ( $\varphi = 3 \text{ cm}$ , thickness  $0.5 \text{ mm}$ ) glued with conducting epoxy glue. The sensitivities of the  $x$ - and  $y$ -piezodrives was  $36 \text{ \AA/V}$ . All piezoelements were calibrated using a fine inductance dilatometer-based method. Tips were prepared from tungsten wire. The coarse positioning and approaching is ensured by means of a hand-driven micrometer connected to a set of tube-levers which demagnify the motion of the tip to an increment of  $100 \text{ \AA}$  [8].

To avoid external vibrations the STM unit was placed on a set of three heavy metal plates with rubber inserts and the whole construction rested on sand in a wooden box supported by many tennis balls. Thermal drifts in the STM unit can be reduced by long term thermal stabilization. The STM unit together with the metal plates and a part of the wooden box is presented in Fig. 1.

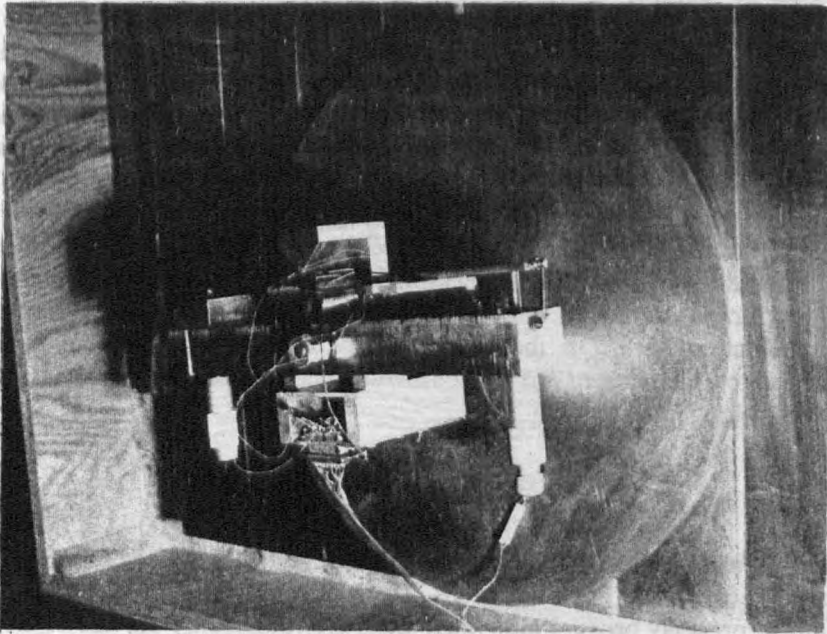


Fig. 1. STM unit—hand-driven micrometers,  $z$ -bimorph with tungsten tip and lever-tube system are seen.

The STM operated in the constant current mode. Stable tunneling current between the sample and the tip is kept constant by a feedback system that pulls or pushes the tip away from or towards the sample. In the WKB approximation the tunneling current through vacuum varies exponentially with the distance  $s$  between the tip and the sample and with the square root of the tunneling barrier height ( $\varphi^{1/2}$ ) according to the formula

$$I = I_0 \exp(-\varphi^{1/2}s).$$

The resulting constant current image reflects the topography of the surface on the assumption that the metal surface is clean, i.e., that  $\varphi$  does not vary greatly compared with the topological changes in the  $z$ -directions.

In our STM unit the feedback system can produce voltages between tip and sample in the range from 1 mV to 3 V giving a tunneling current from 1 nA to 50 nA. The tunneling current and bias voltage can be adapted independently allowing to analyze a wide range of materials ranging from metals to semiconductors. The voltage taken at the output of feedback, which drives the  $z$ -piezodrive to keep the tunneling current constant, is recorded as a function of the tip position and gives the image of the surface investigated. Most of the images were recorded at a tip voltage of 1 V and a tunneling current of 3 nA. Scanning speed along the  $x$ -axis was in the range of hundreds of Å/s. The  $x$  and  $y$  scanning voltages were produced by two ramp generators. Before performing the STM measurements on the  $\text{BiSrCaCu}_2\text{O}_x$  samples, numerous control images of Au and Si surfaces were taken at various surface conditions. Thus, from the ranges of currents and voltages used in the measurements as well as from the noise levels, the metallic nature of the control surfaces could be distinguished from the semiconducting ones. On the basis of these experiments we were able to determine to which class of surfaces the investigated surfaces of our  $\text{BiSrCaCu}_2\text{O}_x$  samples belonged.

#### 4. RESULTS AND DISCUSSION

Figure 2 presents an STM image of an area of  $3600 \text{ \AA} \times 750 \text{ \AA}$  of a  $\text{BiSrCaCu}_2\text{O}_x$  sample at a place where a considerable part of the image reflects a flat surface with terraces and steps. The structure of the steps could not be examined precisely because individual scans are rounded by the size of the tip. However, although the heights of the steps are different: 30, 60, 90 Å, no steps smaller than 30 Å are found. This may suggest that 30 Å corresponds to the dimension of the crystallographic unit cell along the  $z$ -direction found in X-ray analysis.

The image presented in Fig. 3 corresponds to another place on the same surface. The flat terrace-like surfaces with steps are similar to those presented in Fig. 2. The images presented in Figs. 4 and 5 were taken at other places than those

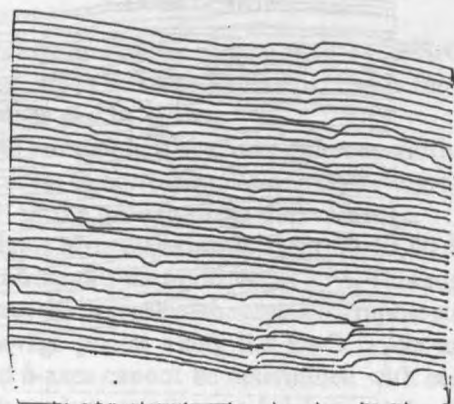


Fig. 2. STM image of a  $\text{BiSrCaCu}_2\text{O}_x$  surface. The units on all axes correspond to 100 Å.

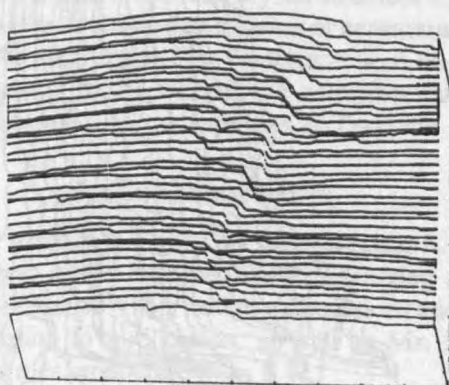


Fig. 3. STM image of a  $\text{BiSrCaCu}_2\text{O}_x$  surface. The units on all axes correspond to 100 Å.

of Figs. 2 and 3. In these Figures similar flat terrace-like surfaces with steps are seen. Only in Fig. 5 in the right-hand lower part a grain boundary or twinning edge is apparent. This edge is seen as a considerable disturbance in the regularity of the picture – the scans suddenly drop down indicating that in this part of the surface the direction of the  $c$ -axis has been changed by  $90^\circ$  as compared with the left-hand part of this picture. In this part at the depths of faults the scans reflect objects which could be identified as surfaces of crystal fracture parallel to the  $c$ -axis. In the fracture the elements of  $30 \text{ \AA}$  multiples can also be distinguished. On the surface of the ceramic  $\text{BiSrCaCu}_2\text{O}_x$  samples many other images were



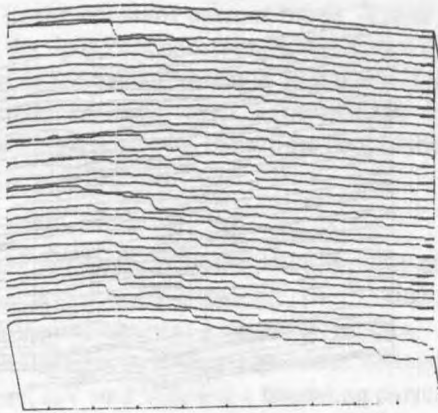


Fig. 4. STM image of a BiSrCaCu<sub>2</sub>O<sub>x</sub> surface. The units on all axes correspond to 100 Å.

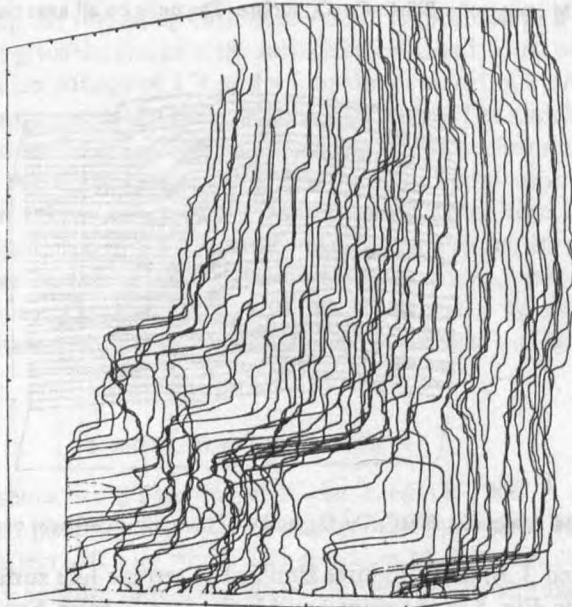


Fig. 5. STM image of a BiSrCaCu<sub>2</sub>O<sub>x</sub> surface. The units on all axes correspond to 100 Å.

observed. Most of them were similar to those presented in Figs. 2–5, but others were more irregular or without well resolved flat terraces. These irregular pictures probably reflect fractures of crystallites in planes not perpendicular to the *c*-axis.

It does not follow either from the analysis of the presented STM images of BiSrCaCu<sub>2</sub>O<sub>x</sub> crystallites or from the symmetry of the orthorhombic structure how to determine the directions of the *a*- and *b*-axes.

## 5. CONCLUSIONS

The most remarkable feature of our surface images of  $\text{BiSrCaCu}_2\text{O}_x$  ceramic samples is the presence of flat terraces and steps. From the analysis of these images several conclusions can be drawn:

(i) Many flat terraces are visible. They have different widths but all have flat parallel surfaces which seem to correspond to one crystallographic plane. These surfaces can be a result of the growth process or cleavage.

(ii) Although the heights of the steps are different, 30, 60, 90 Å, no steps smaller than 30 Å are seen and all heights are multiples of 30 Å. This suggests that 30 Å is the observed dimension of the unit cell of the crystallographic structure. Thus one can speculate that cleavage planes along the Bi-O layers are observed. The directions of the  $a$ - and  $b$ -axes cannot be determined with certainty.

(iii) The correspondence between the step heights and the size of the unit cell along the  $c$ -axis may indicate that the surface of  $\text{BiSrCaCu}_2\text{O}_x$ , although not subjected to special cleaning treatment before the measurements, is rather clean and not covered by any contamination layers deforming its properties because the surface observed at various places seems to be uniform and similar everywhere in its electrical properties. The crystal structure of the bulk material extends to the surface without visible deformation or contamination. This surface inertness may lead to the assumption that the terraces seen on the  $\text{BiSrCaCu}_2\text{O}_x$  surfaces correspond to the (001) plain of the orthorhombic structure along a  $\text{Bi}_2\text{O}_2$  layer in accordance with the assertion of Tarascon *et al.* [9].

## ACKNOWLEDGEMENTS

We wish to thank Professor H. Szymczak and Professor A. Pajęzkowska for their stimulating interest in the Bi-based superconducting materials, Mrs. J. Górecka and Mr. K. Godwod for their valuable discussions and X-ray diffraction data made available prior to publication, as well as Mr. M. Baran for the magnetic susceptibility measurements.

This work was financially supported by the Governmental Programmes RPBP 01.09 and CPBP 01.08.

## REFERENCES

- [1] G. Binning, H. Rohrer, Ch. Gerber and E. Weibel, *Phys. Rev. Lett.* **49**, 57 (1982).
- [2] N. Garcia *et al.*, *Z. Physik* **B70**, 9 (1988).
- [3] L.E.C. van de Leemput, P.J.M. van Bentum, L.W.M. Schreurs and van Kempen, *Physica* **C152**, 99 (1988).
- [4] R. Laiho, L. Heikkila and H. Snellman, *J. Appl. Phys.* **63**, 225 (1988).
- [5] A.M. Okoniewski, J.E. Klemborg-Sapieha and A. Yelon, *Appl. Phys. Lett.* **53**, 151 (1988).
- [6] J. Górecka and K. Godwod, to be published.

[7] D.P.E. Smith, Thesis, Stanford Univ., 1987.  
 [8] A. Witek, A. Dąbkowski and J. Rauuszkiwicz, *Modern Phys. Phys. Lett.* **B3**, 235 (1989).  
 [9] J.M. Tarascon, Y. LePage, P. Barboux, B.G. Bagley, L.H. Green, W.R. McKinnon, G.W. Hull, M. Giroud and D.M. Hwang, *Phys. Rev.* **B37**, 9382 (1988).

example is the presence of the hydrogen in the polymer matrix. Many of the observed phenomena can be explained on the basis of the hydrogen content. (i) Many of the observed phenomena can be explained on the basis of the hydrogen content. (ii) Many of the observed phenomena can be explained on the basis of the hydrogen content. (iii) Many of the observed phenomena can be explained on the basis of the hydrogen content. (iv) Many of the observed phenomena can be explained on the basis of the hydrogen content. (v) Many of the observed phenomena can be explained on the basis of the hydrogen content.

REFERENCES

[1] J. Górecki and J. Górecka, *Polym. Bull.* **1**, 1 (1969).  
 [2] J. Górecki and J. Górecka, *Polym. Bull.* **2**, 1 (1970).  
 [3] J. Górecki and J. Górecka, *Polym. Bull.* **3**, 1 (1971).  
 [4] J. Górecki and J. Górecka, *Polym. Bull.* **4**, 1 (1972).  
 [5] J. Górecki and J. Górecka, *Polym. Bull.* **5**, 1 (1973).  
 [6] J. Górecki and J. Górecka, *Polym. Bull.* **6**, 1 (1974).  
 [7] J. Górecki and J. Górecka, *Polym. Bull.* **7**, 1 (1975).  
 [8] J. Górecki and J. Górecka, *Polym. Bull.* **8**, 1 (1976).  
 [9] J. Górecki and J. Górecka, *Polym. Bull.* **9**, 1 (1977).  
 [10] J. Górecki and J. Górecka, *Polym. Bull.* **10**, 1 (1978).  
 [11] J. Górecki and J. Górecka, *Polym. Bull.* **11**, 1 (1979).  
 [12] J. Górecki and J. Górecka, *Polym. Bull.* **12**, 1 (1980).  
 [13] J. Górecki and J. Górecka, *Polym. Bull.* **13**, 1 (1981).  
 [14] J. Górecki and J. Górecka, *Polym. Bull.* **14**, 1 (1982).  
 [15] J. Górecki and J. Górecka, *Polym. Bull.* **15**, 1 (1983).  
 [16] J. Górecki and J. Górecka, *Polym. Bull.* **16**, 1 (1984).  
 [17] J. Górecki and J. Górecka, *Polym. Bull.* **17**, 1 (1985).  
 [18] J. Górecki and J. Górecka, *Polym. Bull.* **18**, 1 (1986).  
 [19] J. Górecki and J. Górecka, *Polym. Bull.* **19**, 1 (1987).  
 [20] J. Górecki and J. Górecka, *Polym. Bull.* **20**, 1 (1988).